OFFICE OF NAVAL RESEARCH

Contract N7onr-35801

T. O. I.

NR-041-032

Technical Report No. 110

DUCTS FOR ACCELERATED FLOW

by

T. C. Lin

DIVISION OF APPLIED MATHEMATICS

BROWN UNIVERSITY

PROVIDENCE, R. I.

April, 1954

A11-110

DUCTS FOR ACCELERATED FLOW[1]

by

T. C. Lin[2]

ABSTRACT

A method of design for two-dimensional contracting ducts for incompressible and inviscid flow has been developed which gives a rapid change of cross-section with no pressure discontinuity or adverse pressure gradient. While giving essentially uniform flow on both ends it yields ducts of smaller overall length and shorter wall length than those given by existing methods for any contraction ratio. The design is based on a fan-shaped boundary chosen in the hodograph plane, for which the flow is found by conformal mapping. The ducts have a longer inlet portion, part of which may be used as a settling chamber, a short central portion for the acceleration of the flow along the wall, and a short outlet portion, thus cutting down power losses. As examples of the method the design of ducts of contraction ratios 3 and 10 is carried out.

---

1. The results presented in this paper were obtained in the course of research sponsored by the Office of Naval Research under Contract N7onr-35801 with Brown University.

2. Research Associate, Division of Applied Mathematics, Brown University, Providence 12, R. I.

1. Introduction and Summary.

It is of interest in the field of fluid mechanics to determine the shape of the contracting duct that will most effectively increase the velocity of a stream of fluid by a ratio r. In order to reduce the boundary layer effect the wall length of a contracting duct should be as short as possible, while keeping essentially uniform flow on both ends of the duct. In addition these should be no pressure discontinuity or adverse pressure gradient along the wall to cause separation and unsteady conditions.

In the present investigation two-dimensional, irrotational flow is considered. The fluid is assumed to be incompressible and inviscid. For a real fluid the shapes of the contracting ducts should be modified by a slight displacement of the wall outward to allow for the boundary layer thickness. In the case of a compressible medium the compressibility effect on the shapes can be obtained by using the Kármán-Tsien linearized pressure-volume relation.

Methods of design for contracting ducts in two-dimensional irrotational, incompressible and non-viscous flow have been given by various investigators, notably, Hughes [1]*, Cheers [2], Lighthill [3], Whitehead, Wu and Waters [4], and Libbey and Riess [5].

The method by Hughes uses the isobaric lines as the wall of the duct and obtains the most rapid change of cross-section possible without reversal of pressure gradient, but it introduces a spiral singularity and hence a pressure discontinuity along the

* Numbers in square brackets refer to Bibliography at end of paper.

wall, and has to be modified suitably for practical applications. The others avoid the discontinuity defect but fail to make use of the isobaric lines and hence give longer ducts.

Besides, all these methods have the drawback that the maximum angle of the wall of the duct is not adjustable. In Hughes' case the angle of the wall of the duct tends to infinity at the singular point for all contraction ratios and causes the pressure discontinuity, while in all the other cases for a given contraction ratio there is a fixed maximum wall angle, which is either too small or too large to give an optimum shape and leads to ducts longer than necessary.

In the present paper a method of two-dimensional design for contracting ducts is given. Apart from fully utilizing the isobaric lines for the inlet and outlet portions of the wall, it introduces a parameter α for adjusting the maximum wall angle and eliminating the spiral singularity. The advantage of using the isobaric lines is explained in section 2. For a given contraction ratio the optimum α is obtained by minimizing either the overall length of the duct or the length of the wall of the duct. In order to reduce the thickness of the boundary layer, ducts of the shortest wall length are of primary consideration.

While giving essentially uniform flow on both ends and no pressure discontinuity or adverse pressure gradient along the wall, the present method yields ducts of smaller overall length and shortest wall length than those given by existing methods for any contraction ratio. Besides, the ducts have a longer inlet

portion, part of which may be used as a settling chamber, a short central portion for the acceleration of the flow along the wall, and a short outlet portion, thus cutting down power losses. Typical designs are presented for ducts of contraction ratios 3 and 10 as examples of the methods.

Notations.

c, c'	constants, Eqs. (25) and (32)
$f_1 \ldots f_9$	functions, Eqs. (11) to (14), (20) to (22), and (40)
$F(k,\varphi)$	Legendre elliptic integral of the first kind, Eq. (4)
i	$\sqrt{-1}$
Im	Imaginary part of
k	parameter, Eq. (2)
k'	parameter, Eq. (4)
K	$F(k, \pi/2)$, Eq. (4)
K'	$F(k', \pi/2)$, Eq. (4)
r	contraction ratio, Eq. (3)
Re	real part of
s	length of the wall of the duct, Eq. (37)
S	$= \rho e^{i\theta}$, complex variable, Eq. (2)
t	complex variable, Eq. (1)
u,v	velocity components in the x and y-directions
U	velocity upstream of the duct, Eq. (1)
w	$= u - iv$, complex variable in the hodograph plane, Eq. (1)
x,y	Cartesian co-ordinates in the physical plane, Eq. (6)
z	$= x + iy$
α	maximum wall angle, Eq. (2)
α_o	optimum α
γ	$\sin^{-1} k$

γ'	$\sin^{-1} k'$
μ_1, μ_2	velocity deviations at the upstream and downstream ends of the duct, Eqs. (28) and (35)
ν_1, ν_2	permissible velocity deviations at the upstream and downstream ends of the duct, Eq. (49)
θ	angular coordinate in the S-plane, Eq. (2)
ρ	radial distance from the origin in the S-plane, Eq. (2)
φ	parameter
φ_1	$\tan^{-1}(k^{1/2})$, Eq. (37)
ψ	parameter, Eq. (41)
Ω	complex potential function, Eq. (5)

2. The Boundary Shape in the Hodograph Plane.

The shape of the boundary of the duct is first chosen in the hodograph plane, where the co-ordinates are the velocity components u and -v. This is most convenient, for in the hodograph plane, concentric circles centered at the origin are isobaric or constant velocity lines, and straight lines through the origin are lines of constant flow direction.

Assume that the duct is symmetrical with respect to the x-axis, Fig. 1, and has an upstream velocity U, and that the contraction ratio is r. In the hodograph plane, Fig. 2, the upstream end of the duct corresponds to the point A, (U,0), and the downstream end to the point F, (rU,0). All the stream lines start from A and end in F. The axis of symmetry in the physical plane corresponds to the straight line AF in the hodograph plane.

In order to avoid an adverse pressure gradient along the wall of the duct, the boundary in the hodograph plane must lie on or between the two concentric circles of radii U and rU centered at the origin O. If α is the maximum angle between the

wall and the center line of the duct, the boundary in the hodograph plane must lie on or between the two straight lines passing through the origin O and making angles of $\pm\alpha$ with the u-axis. Therefore the boundary in the hodograph plane must lie within the fan-shaped domain or on its boundary. The upper half of the fan-shaped domain is shown in Fig. 2.

From the symmetry of the problem it is only necessary to consider the upper half of the duct. The wall of the duct is conveniently divided into three portions, the inlet BC, the central portion CD, and the outlet DE, Fig. 1. For a short inlet BC it is desirable to turn the flow along the inlet portion of the wall to the maximum wall angle α as fast as possible without increasing the speed of the flow. For a rapid contraction at the central portion it is desirable to increase the speed of the flow along the wall at this maximum angle α as much as possible up to the final speed rU. For a short outlet DE it is desirable to turn the flow along the outlet portion of the wall back to the horizontal direction as fast as possible. It follows from these physical arguments that for ducts of smaller wall length the boundary in the hodograph plane should coincide with the boundary of the fan-shaped domain, Fig. 2.

As a comparison the boundaries used by Whitehead, Wu and Waters, and by Libby and Riess are also shown in Fig. 2. The extreme case that α approaches infinity gives the boundary used by Hughes. The boundaries used by Cheers and Lighthill are compared with the present boundary in Fig. 3.

3. The Mapping Functions.

The flow in the hodograph plane is found by conformal mapping. Let $w = u - iv$ be the complex co-ordinate in the hodograph plane. The upper half of the fan-shaped domain in the w-plane, Fig. 2, is mapped into the rectangle in the t-plane, Fig. 3, by the equation

$$w = U e^{t}, \tag{1}$$

where $1 \leq |W|/U \leq r$, $0 \leq \text{Arg } w \leq \alpha$, and $0 \leq \text{Re } t \leq \ln r$, $0 \leq \text{Im } t \leq \alpha$.

The rectangle in the t-plane is mapped into the upper half of the S-plane, Fig. 4, by the equation,

$$t = \frac{\alpha}{2K} \int_0^S \frac{dS}{\sqrt{S(S + k)(kS + 1)}}, \quad S = \rho e^{i\Theta}, \tag{2}$$

where $\text{Im } S \geq 0$. The parameter k is related to the contraction ratio r and the maximum wall angle α by the equation

$$\ln r = \alpha K'/K \tag{3}$$

where K and K' are complete Legendre elliptic integrals of the first kind defined by

$$\left.\begin{aligned} K &= F(k, \pi/2), \\ K' &= F(k', \pi/2), \\ F(k,\varphi) &= \int_0^{\varphi} \frac{d\varphi}{\sqrt{1 - k^2 \sin^2 \varphi}}, \\ k'^2 &= 1 - k^2. \end{aligned}\right\} \tag{4}$$

It is readily seen that K'/K is a function of k or k' only. The values of K'/K for various values of k or k' are given in tables of complete elliptic integrals.

The complex potential function for the upper half of the S-plane with a source at the origin and a sink at infinity is simply

$$\Omega = (U/\pi) \ln S. \tag{5}$$

The strength of the source, U/π, is chosen to yield a half width of unity for the entrance of the duct.

If $z = x + iy$ is the complex co-ordinate in the physical plane, one has

$$z = \int \frac{d\Omega}{w} \tag{6}$$

Eliminating w, t, and Ω between Eqs. (1), (2), (5), and (6) yields

$$z = \frac{1}{\pi} \int_{1/k}^{S} \frac{dS}{S} \operatorname{Exp} \left[- \frac{\alpha}{2K} \int_{0}^{S} \frac{dS}{\sqrt{S(S + k)(kS + 1)}} \right]. \tag{7}$$

The lower limit $1/k$ of the above integral is chosen for mathematical simplicity and to fix the origin of the z-plane on the center line and close to the throat of the duct.

4. The Boundary Shape in the Physical Plane.

As S varies from zero to minus infinity along the negative real axis, z traces along one branch of the boundary of the duct from the upstream end to the downstream end. Putting $S = -\rho$, using the appropriate limits, and separating the real and imaginary parts, one obtains from Eq. (7) the following equations for the boundary of the duct in the physical plane in terms of the parameter φ.

For the inlet BC:

$$\left.\begin{aligned} x - x_C &= -[f_1(k, \alpha, \varphi) - f_2(k, \alpha, \varphi)], \\ y - y_C &= f_3(k, \alpha, \varphi), \end{aligned}\right\} \tag{8}$$

where $0 \leq \varphi \leq \pi/2$, and $\cos^2 \varphi = \rho/k$.

For the central straight portion CD:

$$\left.\begin{aligned} x_C - x_D &= - f_4(k', r, \pi/2)\cos \alpha, \\ y_C - y_D &= f_4(k', r, \pi/2)\sin \alpha. \end{aligned}\right\} \tag{9}$$

For the outlet DE:

$$\left.\begin{aligned} x_D - x &= - \frac{1}{r}[f_1(k, \alpha, \varphi) - f_2(k, \alpha, \varphi)], \\ y_D - y &= \frac{1}{r} f_3(k, \alpha, \varphi), \end{aligned}\right\} \tag{10}$$

where $0 \leq \varphi \leq \pi/2$, and $\sec^2 \varphi = k\rho$.

A comparison of Eqs. (8) and (10) shows that the inlet and outlet portions of the wall follow the same geometrical curve and differ only by a scale factor 1/r. The half widths of the duct at the upstream end and the downstream end approach asymptotically to 1 and 1/r, respectively.

In the above the functions f's are defined as follows:

$$f_1(k, \alpha, \varphi) = \frac{2}{\pi} \cos[\alpha F(k, \tfrac{\pi}{2} - \varphi)/K] \ln \sec \varphi, \tag{11}$$

$$f_2(k, \alpha, \varphi) = \frac{2\alpha}{\pi K} \int_0^{\varphi} \frac{\sin[\alpha F(k, \tfrac{\pi}{2} - \varphi)/K] \ln \sec \varphi \, d\varphi}{(1 - k^2 \cos^2 \varphi)^{1/2}}, \tag{12}$$

$$f_3(k, \alpha, \varphi) = \frac{2}{\pi} \int_0^{\varphi} \sin[\alpha F(k, \tfrac{\pi}{2} - \varphi)/K] \tan \varphi \, d\varphi, \tag{13}$$

$$f_4(k', r, \varphi) = \frac{k'^2}{\pi} \int_0^{\varphi} \frac{r^{-[1 - F(k', \frac{\pi}{2} - \varphi)/K']} \sin 2\varphi \, d\varphi}{1 - k'^2 \cos^2 \varphi} \tag{14}$$

These integrals can be evaluated without difficulty.

5. The Velocity Distribution.

Combining Eqs. (1) and (2) gives the expression for the velocity in terms of S:

$$w = U \, \mathrm{Exp}\left[\frac{\alpha}{2K}\int_0^S \frac{dS}{\sqrt{S(S+k)(kS+1)}}\right], \quad S = \rho e^{i\theta}, \tag{15}$$

where $\mathrm{Im}\, S \geq 0$, $1 \leq |w|/U/U \leq r$, and $0 \leq \mathrm{Arg}\, w \leq \alpha$.

Consider first the velocity distribution along the wall of the duct. From the boundary chosen in the hodograph plane it is clearly seen that along the inlet BC

$$|w| = U, \tag{16}$$

and along the outlet DE

$$|w| = rU. \tag{17}$$

Therefore along the wall of the duct the acceleration of the fluid takes place only along the central straight portion CD. Using the condition $\theta = \pi$, one obtains from Eqs. (15) and (7) the velocity distribution along CD in terms of the parameter φ as follows:

$$\left.\begin{aligned} |w|/U &= f_5(k',r,\varphi), \\ |z - z_C| &= f_4(k',r,\varphi), \end{aligned}\right\} \tag{18}$$

where $0 \leq \varphi \leq \pi/2$, and $\cos^2\varphi = (1 - k\rho)/(1 - k^2)$.

Similarly, using the condition $\theta = 0$, one obtains the velocity distribution along the center line of the duct,

$$\left.\begin{aligned} u/U &= f_5(k',r,\varphi), \\ x &= f_6(k',r,\varphi) - f_7(k',r,\varphi), \end{aligned}\right\} \tag{19}$$

where $0 \leq \varphi \leq \pi/2$, and $\tan^2\varphi = k\rho$. From symmetry, v is zero along the center line.

In the above, f_4 is defined by Eq. (14); f_5, f_6, and f_7 are defined as follows:

$$f_5(k',r,\varphi) = r^{[1 - F(k', \frac{\pi}{2} - \varphi)/K']} \tag{20}$$

$$f_6(k',r,\varphi) = \frac{2}{\pi} r^{-[1 - F(k', \frac{\pi}{2} - \varphi)/K']} \ln \tan \varphi, \tag{21}$$

$$f_7(k',r,\varphi) = \frac{2 \ln r}{\pi K'} \int_{\pi/4}^{\varphi} \frac{r^{-[1-F(k', \frac{\pi}{2} - \varphi)/K']} \ln \tan \varphi \, d\varphi}{(1 - k'^2 \cos^2 \varphi)^{1/2}} \tag{22}$$

Consider next the velocity distribution at the upstream end of the duct. At the upstream end

$$|S|/k \ll 1. \tag{23}$$

On neglecting S/k and its higher powers as compared to 1, and since α/K is of the order 1 or less, Eqs. (15) and (7) reduce, respectively, to

$$w/U = 1 - (\alpha/K)(S/k)^{1/2}, \tag{24}$$

and

$$z = -\frac{1}{\pi}[\ln(k/S) + 2(\alpha/K)(S/k)^{1/2}] + c. \tag{25}$$

Here c is a real constant and its value, in general, depends on the two parameters k and α.

Separating the real and imaginary parts of Eqs. (24) and (25) yields

$$\left.\begin{aligned} u/U &= 1 - (\alpha/K)(\rho/k)^{1/2} \cos(\theta/2), \\ v/U &= -(\alpha/K)(\rho/k)^{1/2} \sin(\theta/2), \end{aligned}\right\} \tag{26}$$

and

$$\left.\begin{aligned} x &= -\frac{1}{\pi}[\ln(k/\rho) + 2(\alpha/K)(\rho/k)^{1/2} \cos(\theta/2)] + c, \\ y &= \frac{1}{\pi}[\theta - 2(\alpha/K)(\rho/k)^{1/2} \sin(\theta/2)], \end{aligned}\right\} \tag{27}$$

where $\rho/k << 1$, and $0 \leq |\theta| \leq \pi$. From symmetry θ is negative for the lower half of the duct.

Denoting the velocity deviation at the upstream end of the duct by

$$\mu_1 = |w - U|/U, \tag{28}$$

which is a measure of the ratio of the undesirable velocity deviation to the uniform velocity at the upstream end, one has from Eq. (24)

$$\mu_1 = (\alpha/K)(\rho/k)^{1/2}, \tag{29}$$

where $\rho/k \ll 1$. From Eqs. (27) it is readily seen that for constant x the maximum ρ occurs at $y = \theta = 0$. It follows from Eq. (29) that at the upstream end of the duct for constant x the maximum μ_1 occurs at the center line of the duct.

Similarly, at the down stream end of the duct

$$1/(k|S|) << 1, \tag{30}$$

and Eqs. (15) and (7) reduce to

$$w/rU = 1 - (\alpha/K)(kS)^{-1/2}, \tag{31}$$

and

$$z = \frac{1}{\pi r}\left[\ln(kS) + 2(\alpha/K)(kS)^{-1/2}\right] + c', \tag{32}$$

where c' is a real constant. Separating the real and imaginary parts yields

$$\left.\begin{aligned} u/rU &= 1 - (\alpha/K)(k\rho)^{-1/2}\cos(\theta/2), \\ v/rU &= -(\alpha/K)(k\rho)^{-1/2}\sin(\theta/2). \end{aligned}\right\} \tag{33}$$

and

$$\left.\begin{aligned} x &= \frac{1}{\pi r}[\ln(k\rho) + 2(\alpha/K)(k\rho)^{-1/2}\cos(\theta/2)] + c', \\ y &= \frac{1}{\pi r}[\theta - 2(\alpha/K)(k\rho)^{-1/2}\sin(\theta/2)], \end{aligned}\right\} \quad (34)$$

where $1/k\rho \ll 1$ and $0 \leq |\theta| \leq \pi$.

Similarly, denoting the velocity deviation at the downstream end of the duct by

$$\mu_2 = |w - rU|/rU, \quad (35)$$

one has from (31)

$$\mu_2 = (\alpha/K)(k\rho)^{-1/2}, \quad (36)$$

where $1/k\rho \ll 1$. From Eq. (34) it is readily seen that for constant x, the minimum ρ occurs at $y = \theta = 0$. It follows from Eq. (36) that at the downstream end of the duct for constant x the maximum μ_2 occurs at the center line of the duct.

The velocity distribution across the central section of the duct is well illustrated by the isobaric and equal-velocity potential line LM, Fig. 1. The line LM corresponds to the upper half of the unit circle in the S-plane, Fig. 4.

The point L lies on the center-line of the duct. Putting $\rho = 1$, one obtains from Eq. (19)

$$\left.\begin{aligned} x_L &= f_6(k',r,\varphi_1) - f_7(k',r,\varphi_1) \\ \varphi_1 &= \tan^{-1}(k^{1/2}) \end{aligned}\right\} \quad (37)$$

Along the line LM $\rho = 1$; Eqs. (15) and (7) yield, respectively,

$$|w|/U = r^{1/2} \quad (38)$$

and

$$\left.\begin{aligned} x - x_L &= r^{-1/2}\, f_8(k,\alpha,\varphi) \\ y &= r^{-1/2}\, f_9(k,\alpha,\varphi) \end{aligned}\right\} \tag{39}$$

where

$$\left.\begin{aligned} f_8(k,\alpha,\varphi) &= \frac{2}{\pi}\int_0^{\varphi} \sin\left[\frac{\alpha}{(1+k)K}\, F\left(\frac{2k^{1/2}}{1+k},\, \varphi\right)\right] d\varphi \\ f_9(k,\alpha,\varphi) &= \frac{2}{\pi}\int_0^{\varphi} \cos\left[\frac{\alpha}{(1+k)K}\, F\left(\frac{2k^{1/2}}{1+k},\, \varphi\right)\right] d\varphi \end{aligned}\right\} \tag{40}$$

$0 \le \varphi = \frac{\theta}{2} \le \frac{\pi}{2}$, and $\varphi = \frac{\pi}{2}$ at the point M. On using Landen's Transformation [6],

$$\left.\begin{aligned} \tan\psi &= \frac{\sin 2\varphi}{k + \cos 2\varphi}, \\ F\left(\frac{2k^{1/2}}{1+k}, \varphi\right) &= \frac{1+k}{2}\, F(k,\psi), \end{aligned}\right\} \tag{41}$$

since $\psi = \pi$ for $\varphi = \pi/2$, it follows that

$$\frac{1}{(1+k)K}\, F\left(\frac{2k^{1/2}}{1+k}, \frac{\pi}{2}\right) = 1 \tag{42}$$

The distance CM is obtained from Eq. (18) by putting $\rho = 1$,

$$\left.\begin{aligned} |z_C - z_M| &= f_4(k', r, \varphi_1) \\ \varphi_1 &= \tan^{-1}(k^{1/2}) \end{aligned}\right\} \tag{43}$$

6. The Length of the Wall and the Optimum α.

Let s denote the length of the wall of the duct. Since on the wall $|\Theta| = \pi$, Eqs. (5) and (6) yield

$$s = \int |dz| = \frac{U}{\pi}\int \frac{d\rho}{\rho w}. \tag{44}$$

Along the inlet BC $|w| = U$, and Eq. (44) gives

$$s_{BC} = \frac{1}{\pi} \ln(k/\rho_B), \tag{45}$$

where $0 \leq \rho_B/k \leq 1$. Similarly, along the outlet DE $|w| = rU$, and

$$s_{DE} = \frac{1}{\pi r} \ln(k\rho_E), \tag{46}$$

where $0 \leq 1/k\rho_E \leq 1$. From Eqs. (9),

$$s_{CD} = f_4(k', r, \pi/2). \tag{47}$$

Therefore the total length of the wall from B to E is

$$s_{BE} = \frac{1}{\pi}[\ln(k/\rho_B) + \frac{1}{r} \ln(k\rho_E)] + f_4(k', r, \pi/2). \tag{48}$$

So far α is still undetermined, but it is related to the contraction ratio r and the parameter k or k' by Eqs. (3) and (4). For a given r one may assume a value for α and find the corresponding value of k' from Eqs. (3) and (4). In general, however, for a given contraction ratio r with a given set of permissible velocity deviations v_1 and v_2 at the two ends of the duct, there is an optimum α and hence an optimum k' that will give a shortest wall length for the duct. This is most desirable as it will minimize the boundary layer effect to the flow.

In order to determine the optimum α or k' it is necessary to express the length of the wall in terms of the contraction ratio r, the permissible velocity deviations v_1 and v_2, and α or k'. Let H and G denote respectively the two points at the upstream and downstream ends and on the center line of the duct, Fig. 1. Since the maximum velocity deviations on both ends of the duct always occur at the center line, it follows from Eqs. (29) and (36), that

$$\left.\begin{aligned} \nu_1 &= (\alpha/K)(\rho_H/k)^{1/2}, \\ \nu_2 &= (\alpha/K)(\rho_G k)^{-1/2}. \end{aligned}\right\} \tag{49}$$

Using the condition that the value of θ is zero at the center line and π at the upper wall, one has from Eqs. (27) and (34),

$$\left.\begin{aligned} \ln(k/\rho_B) &= \ln(k/\rho_H) + 2(\alpha/K)(\rho_H/k)^{1/2} \\ \text{and} \quad \ln(k\rho_E) &= \ln(k\rho_G) + 2(\alpha/K)(k\rho_G)^{-1/2}, \end{aligned}\right\} \tag{50}$$

which, in view of Eqs. (49) and (3), become

$$\left.\begin{aligned} \ln(k/\rho_B) &= 2[\nu_1 + \ln(\frac{\ln r}{\nu_1 K'})] \\ \text{and} \quad \ln(k\rho_E) &= 2[\nu_2 + \ln(\frac{\ln r}{\nu_2 K'})]. \end{aligned}\right\} \tag{51}$$

Substituting these into Eq. (48) gives the length of the wall in terms of r, ν_1, ν_2 and k' as follows.

$$s_{BE} = \frac{2}{\pi}[\nu_1 + \ln\frac{1}{\nu_1} + \frac{1}{r}(\nu_2 + \ln\frac{1}{\nu_2}) - (1 + \frac{1}{r})\ln(\frac{K'}{\ln r})] + f_4(k', r, \pi/2). \tag{52}$$

Equation (52) holds for ν_1 and ν_2 small, which is the case of practical interest. Both ln K' and $f_4(k', r, \pi/2)$ increase with k', and for a given r there is an optimum k' and hence an optimum α which gives the shortest wall. Minimizing Eq. (52) one obtains the optimum k', and hence from Eqs. (3) and (4) the optimum α. The latter is platted against r in Fig. 5. As a comparison the α's given by the other methods are also shown in the same figure. The variation of $\sin^{-1} k$ against the compression ratio r for

various values of α is shown in Fig. 5a. The variations of k, k', K, K', K/K' and K'/K against γ and γ' are shown in Fig. 5b, where $\gamma = \sin^{-1} k$ and $\gamma' = \sin^{-1} k'$.

7. Examples.

Calculation of the shape of the boundary has been made for the contraction ratios r = 3 and 10 using the corresponding optimum α's. The results are given in Tables 1, 1a, and 2, 2a, and are illustrated in Figures 6, 6a, 6b and 7, 7a, 7b, respectively.

8. Conclusion and Discussion.

Using the constant velocity lines as the inlet and outlet portions of the wall and introducing a parameter α for adjusting the maximum wall angle, the present method yields, for all contraction ratios, contracting ducts of shorter wall length and smaller overall length than those given by existing methods with no pressure discontinuity or adverse pressure gradient.

The ducts have a longer inlet portion, part of which may be used as a settling chamber, a short central portion for the acceleration of the flow along the wall, and a short outlet portion, thus cutting down power losses.

Physical arguments and numerical results indicate the wall of the duct given by the present method to be the shortest possible without pressure discontinuity or adverse pressure gradient.

The present investigation may be extended to ducts with a certain allowable adverse pressure gradient or ducts with parallel walls on one or both ends by shifting the locations of the source and sink in the S-plane along the positive real axis.

For a compressible medium the effect of compressibility on the shape of the ducts may be obtained by using the Kármán-Tsien linearized pressure-volume relation.

Boundary shpaes which are satisfactory for two-dimensional ducts will, in general, have some extra margin of safety for the pressure gradient when used for tunnels of circular cross section, in spite of the larger contraction ratio [4]. Making use of the close similarity between the shapes of the stream lines for the two flows, this can readily be checked for any particular case when the two-dimensional solution is known. In comparison with the ducts for axi-symmetric flow given by Whitehead, Wu, and Waters [4], it is expected that the present design when used for tunnels of circular cross-section will also offer a shorter wall.

Flow through Y-shaped channels with the same contraction ratio as the ducts and with no adverse pressure gradient can be obtained by shifting the source from the point A to C in the S-plane, and making use of the symmetry of the problem. One half of the Y-shaped channels yields the elbows for accelerated flow given by Carrier [7].

Similarly, flow through inverted Y-shaped channels can be obtained by keeping the source at A and shifting the sink from F to D in the S-plane. This method can be generalized to study flow through an intersection of several channels of various velocity ratios and at various angles.

REFERENCES

1. Hughes, N. J. S. (1944), "Stream Expansion with a Discontinuity in velocity on the boundary", R. &. M. 1978, 1944.
2. Cheers, F. (1945), "Note on Wind Tunnel Contractions", R. & M. 2137, 1945.
3. Lighthill, M. J. (1945), "A New Method of Two-dimensional Aerodynamic Design", R. &. M. 2212, 1945.
4. Whitehead, L. G., Wu, L. Y. and Waters, M. H. L. (1951), "Contracting Ducts of Finite Length", The Aeronautical Quarterly, London Royal Aeronautical Society, Vol. II, Part IV, Feb. 1951.
5. Libby, P. A., and Reiss, H. R., (1951), "The Design of Two-Dimensional Contraction Sections", Quart. of Applied Math., Vol. IX, No. 1, 1951.
6. McRobert, T. M., "Functions of a Complex Variable", MacMillan and Co., Ltd., London, England, 3rd ed., p. 174.
7. Carrier, G. F., (1947), "Elbows for Accelerated Flow", Journal of Applied Mechanics, Vol. 14, No. 2, 1947.

TABLE 1

Values of f_1, f_2, f_3, f_8 and f_9 for r = 3

with $\sin^{-1} k = 41^\circ$, i.e., $\alpha = 59^\circ$

φ°	f_1	f_2	$f_1 - f_2$	f_3	f_8	f_9
0	0	0	0	0	0	0
10	.006	.000	.006	.008	.003	.111
20	.029	.003	.026	.030	.014	.222
30	.073	.008	.065	.063	.031	.331
40	.147	.016	.131	.106	.056	.440
50	.258	.027	.231	.156	.089	.505
60	.421	.041	.380	.212	.132	.649
70	.669	.055	.614	.272	.186	.745
80	1.109	.068	1.041	.334	.255	.833
83	1.336	.071	1.265	.353	.278	.864
86	1.693	.073	1.620	.372	.304	.878
89	2.575	.075	2.500	.391	.313	.904
90	∞	.075	∞	.398	.341	.910

TABLE 1a

Values of f_4, f_5, f_6 and f_7 for r = 3

with $\sin^{-1} k' = 49^\circ$, i.e. $\alpha = 59^\circ$.

φ	f_4	f_5	f_6	f_7	$f_6 - f_7$
0	0	1.000	$-\infty$	.419	$-\infty$
1	.000	1.015	-2.537	.370	-2.907
2	.001	1.031	-2.072	.336	-2.408
3	.001	1.047	-1.793	.306	-2.099
4	.002	1.063	-1.594	.281	-1.875
6	.004	1.096	-1.309	.237	-1.546
8	.008	1.135	-1.101	.201	-1.302
10	.011	1.164	- .950	.170	-1.120
15	.023	1.253	- .669	.113	- .782
20	.037	1.346	- .478	.068	- .546
25	.053	1.443	- .337	.038	- .375
30	.069	1.544	- .227	.020	- .247
35	.084	1.647	- .138	.008	- .146
40	.098	1.753	- .064	.002	- .066
45	.111	1.862	0	0	0
50	.122	1.974	.057	.002	.055
55	.131	2.088	.109	.006	.103
60	.139	2.205	.159	.014	.145
65	.146	2.326	.209	.023	.186
70	.151	2.451	.263	.036	.227
75	.155	2.580	.325	.051	.274
80	.157	2.714	.407	.069	.338
83	.158	2.797	.477	.083	.394
86	.159	2.882	.588	.098	.490
89	.159	2.970	.868	.120	.748
90	.159	3.000	∞	.130	∞

TABLE 2

Values of f_1, f_2, f_3, f_8 and f_9 for r = 10 with $\sin^{-1} k = 13^\circ$, i.e., $\alpha = 72.3^\circ$

φ°	f_1	f_2	f_1-f_2	f_3	f_8	f_9
0	0	0	0	0	0	0
10	.004	.000	.004	.009	.006	.111
20	.022	.003	.019	.035	.027	.220
30	.061	.010	.051	.076	.057	.327
40	.130	.023	.107	.129	.103	.429
50	.239	.041	.198	.194	.158	.524
60	.404	.064	.340	.268	.230	.610
70	.657	.089	.568	.349	.311	.685
80	1.104	.114	.990	.435	.406	.745
83	1.334	.120	1.214	.461	.436	.759
86	1.692	.124	1.568	.487	.467	.772
89	2.575	.127	2.448	.514	.498	.784
90	∞	.127	∞	.523	.508	.788

TABLE 2a

Values of f_4, f_5, f_6 and f_7 for $r = 10$, with $\sin^{-1} k' = 77^\circ$, i.e. $\alpha = 72.3^\circ$

φ	f_4	f_5	f_6	f_7	f_7-f_6
0	0	1.000	$-\infty$	1.049	$-\infty$
1	.003	1.063	-2.424	.851	-3.275
2	.007	1.131	-1.889	.720	-2.609
3	.015	1.201	-1.562	.607	-2.169
4	.024	1.275	-1.329	.531	-1.860
6	.047	1.430	-1.003	.397	-1.400
8	.073	1.594	- .784	.302	-1.086
10	.099	1.766	- .626	.232	- .858
15	.158	2.211	- .379	.121	- .500
20	.203	2.667	- .241	.063	- .304
25	.238	3.127	- .155	.032	- .187
30	.263	3.590	- .097	.015	- .112
35	.282	4.054	- .056	.006	- .062
40	.297	4.523	- .025	.001	- .026
45	.309	4.996	0	0	0
50	.318	5.478	.020	.001	.019
55	.325	5.970	.038	.004	.034
60	.330	6.476	.054	.007	.047
65	.334	6.997	.069	.012	.057
70	.337	7.541	.085	.018	.067
75	.339	8.106	.103	.025	.078
80	.340	8.702	.127	.033	.094
83	.341	9.074	.147	.039	.108
86	.341	9.460	.179	.045	.134
89	.341	9.863	.261	.054	.207
90	.341	10.000	∞	.059	∞

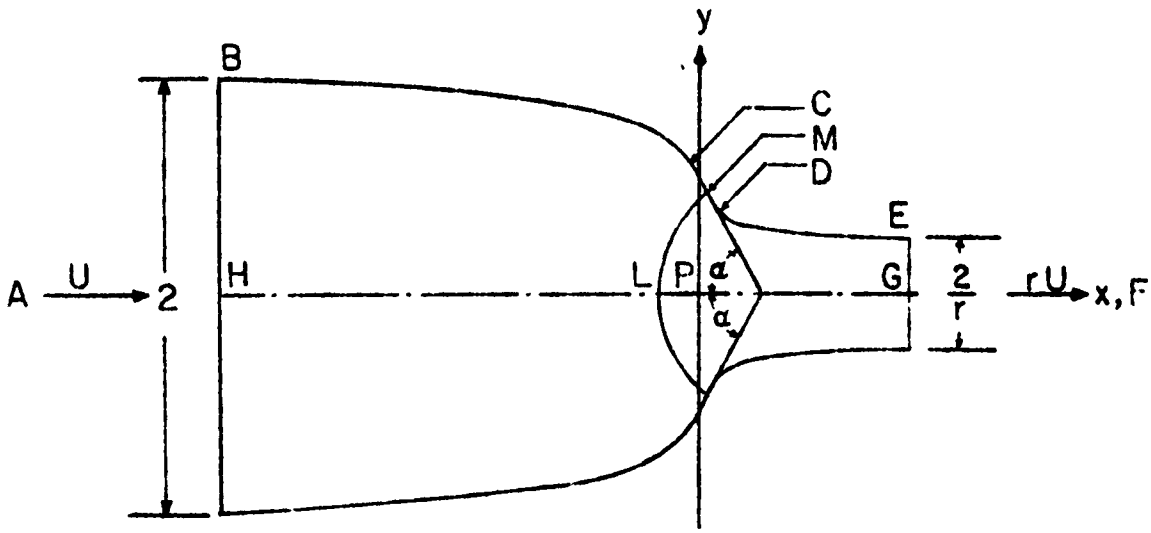

FIG. 1, z-PLANE, THE DUCT

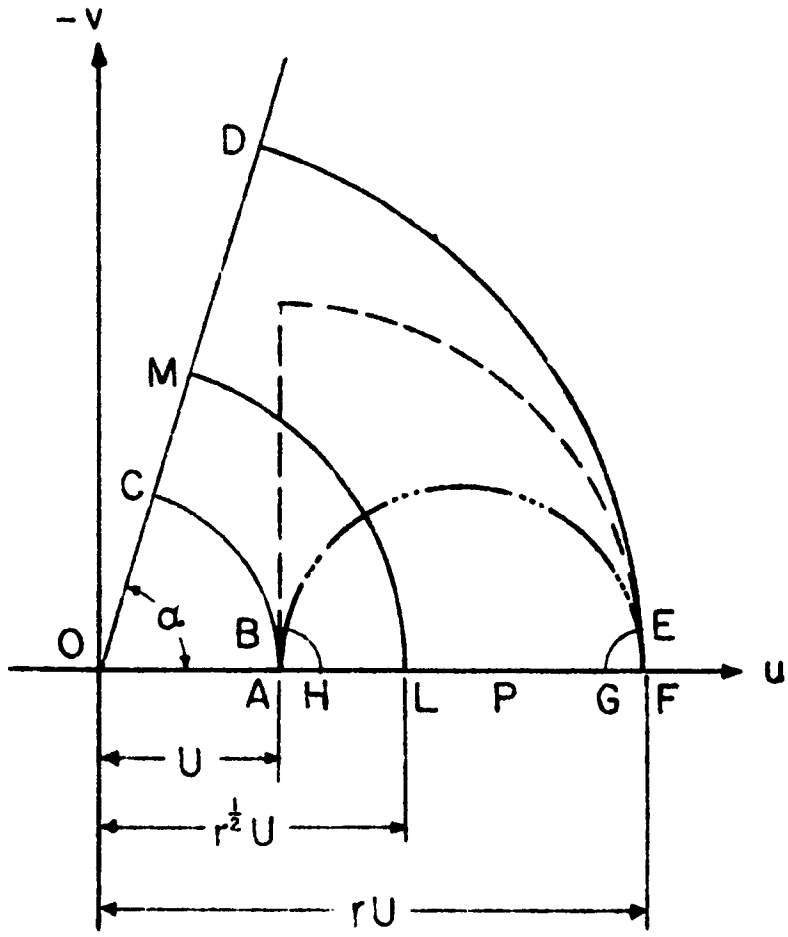

FIG. 2, THE HODOGRAPH PLANE,

w-PLANE

ABCDEF present method

— — — Whitehead, Wu and Waters

—·—·— Libby and Reiss

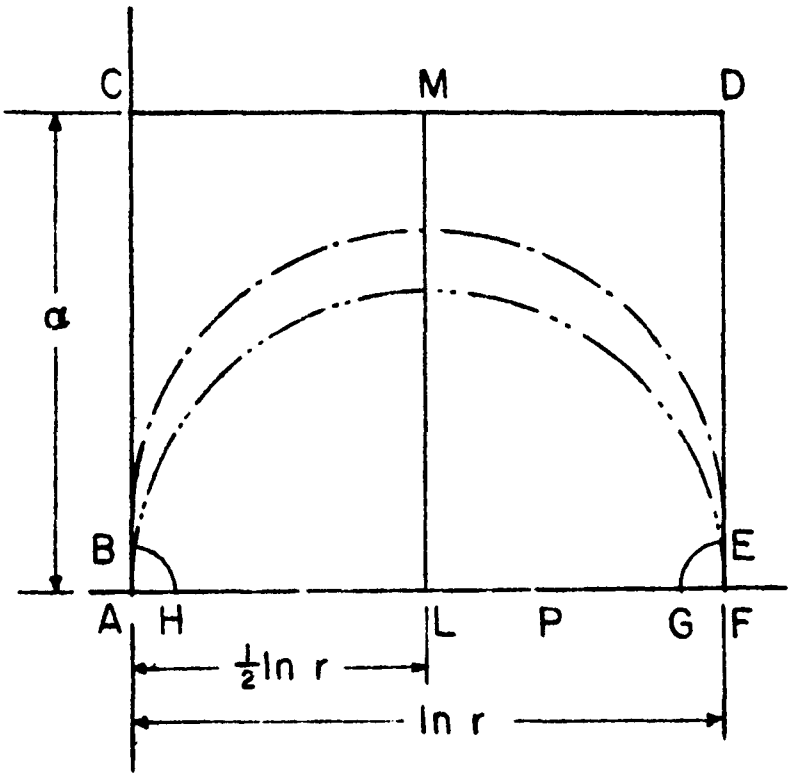

FIG. 3, t— PLANE

ABCDEF present method
—·— Lighthill
—··— Cheers

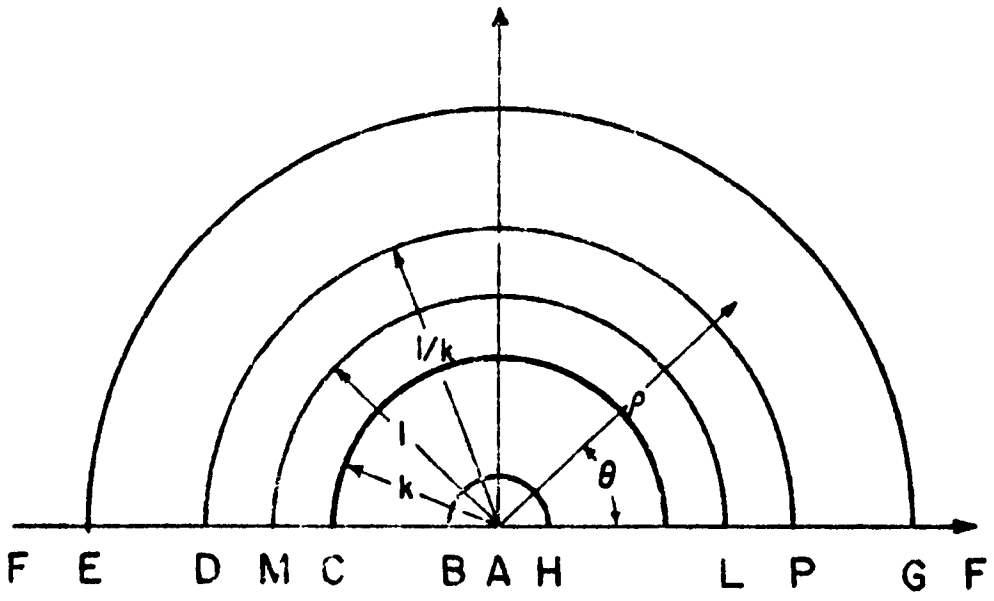

FIG. 4, S-PLANE

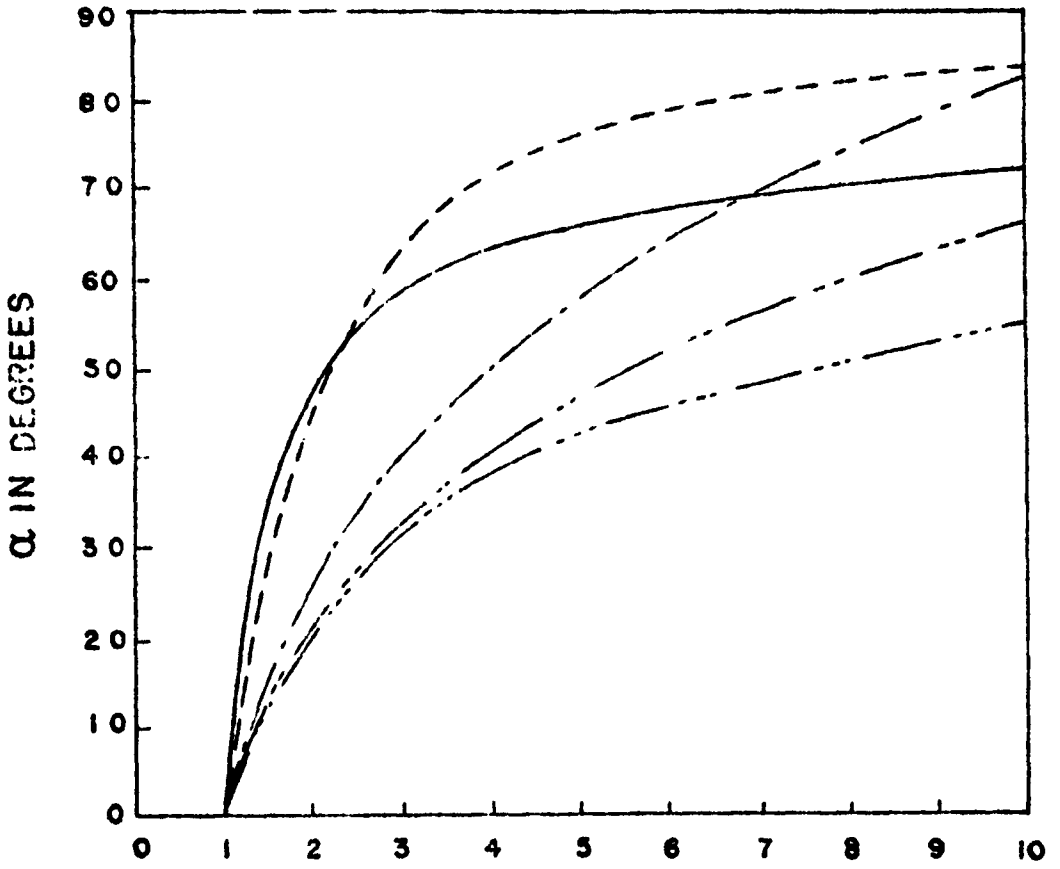

FIG. 5, COMPARISON OF MAXIMUM WALL ANGLE FOR DIFFERENT METHODS

——— Present method with $\alpha = \alpha_o$
– – – – Whitehead, Wu and Waters
—.—.—. Lighthill
—..—..— Cheers
—...—... Libby and Reiss

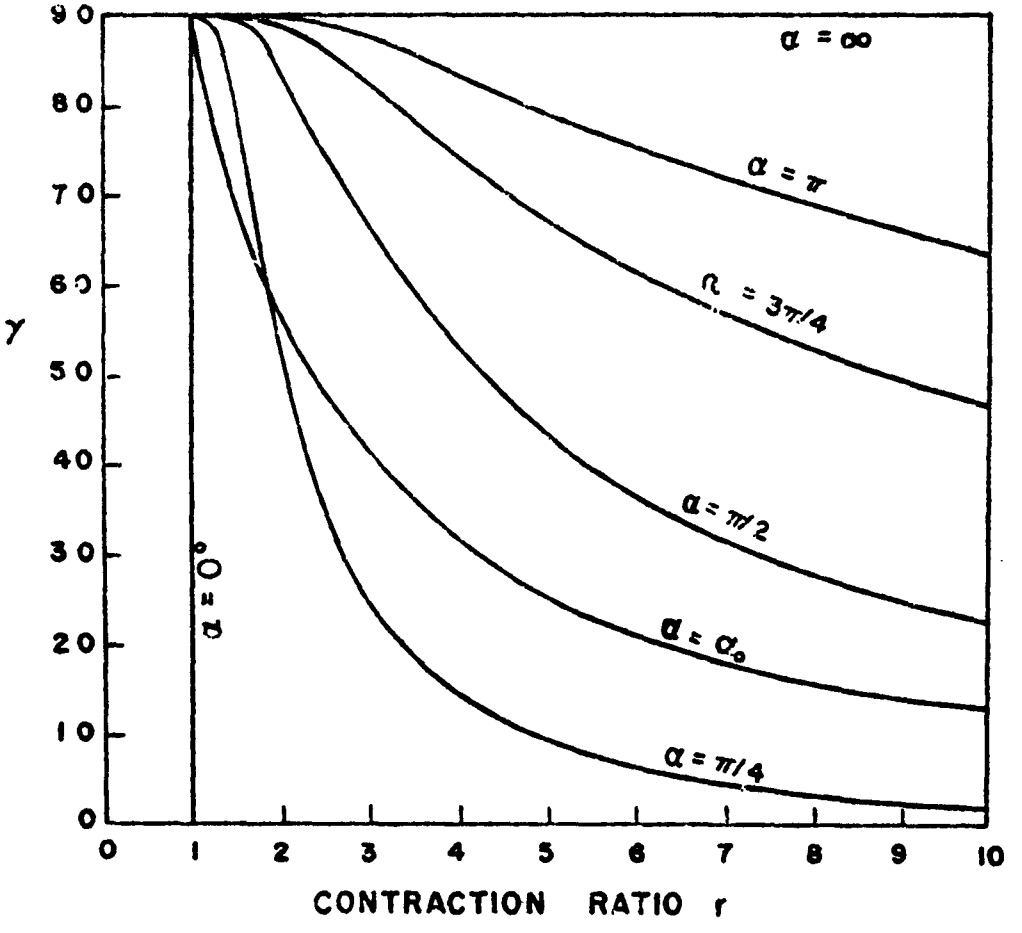

FIG. 5a, γ AGAINST r FOR VARIOUS VALUES OF α

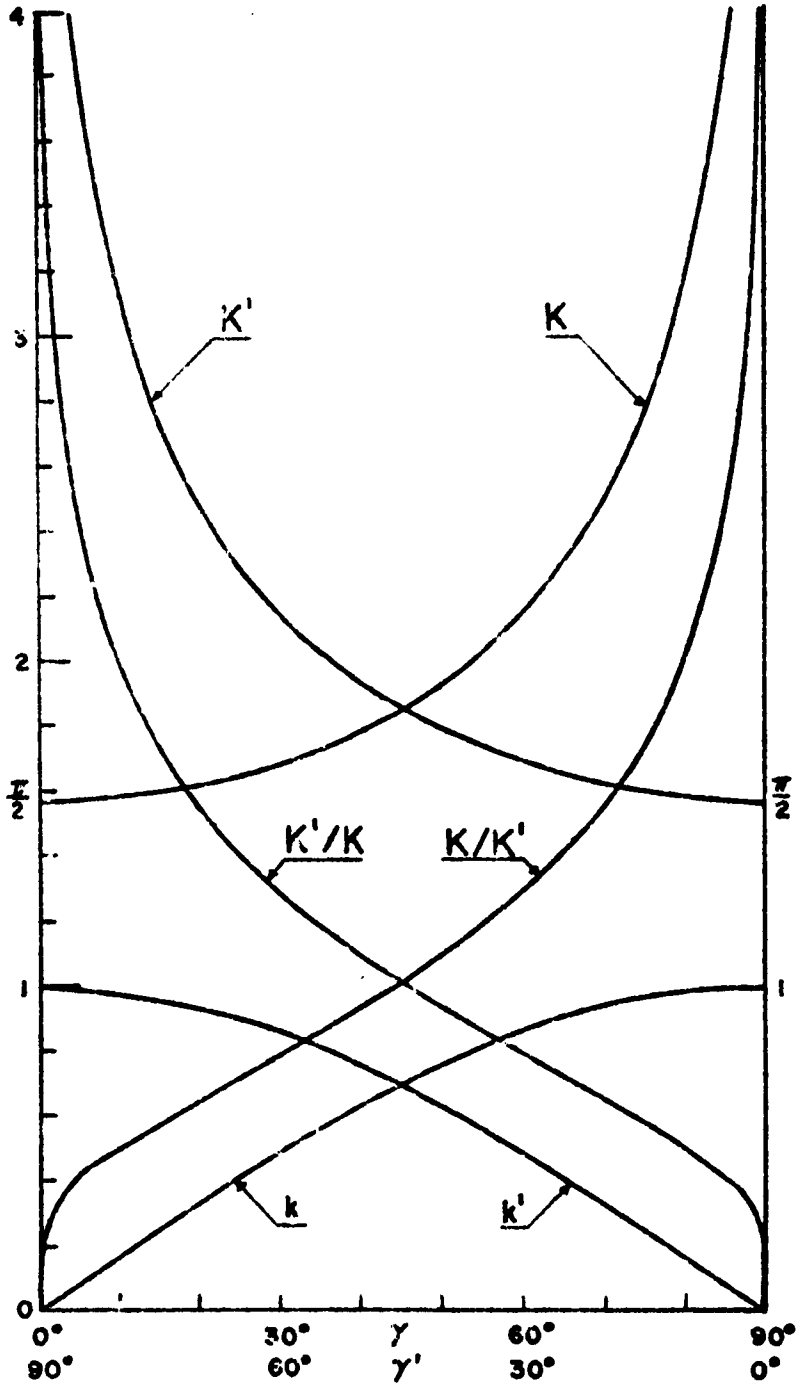

FIG. 5b, k, k', K, K', K/K', K'/K AGAINST γ AND γ'

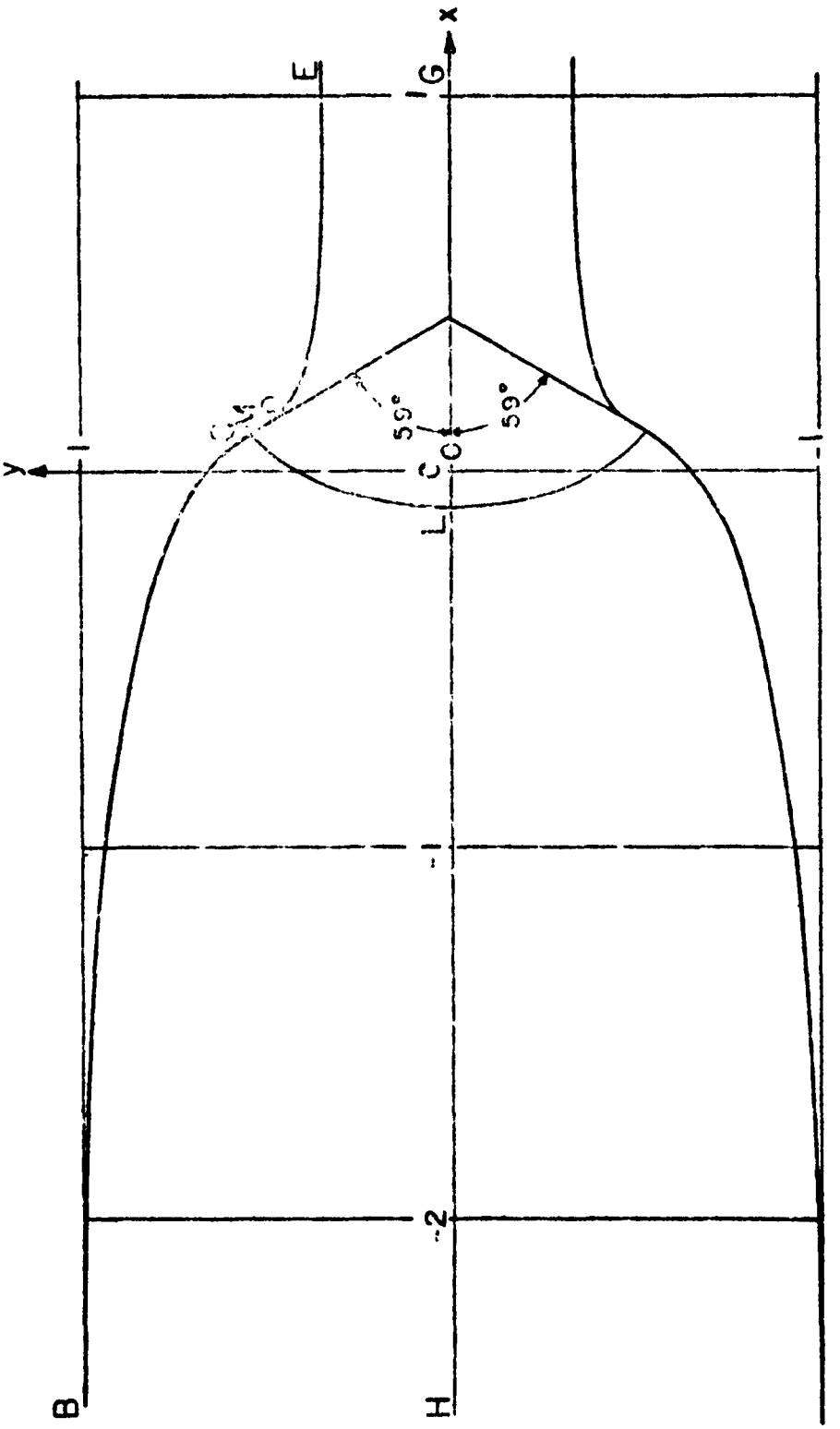

FIG. 6, 3:1 CONTRACTING DUCT WITH $\alpha = \sigma$, (59°)

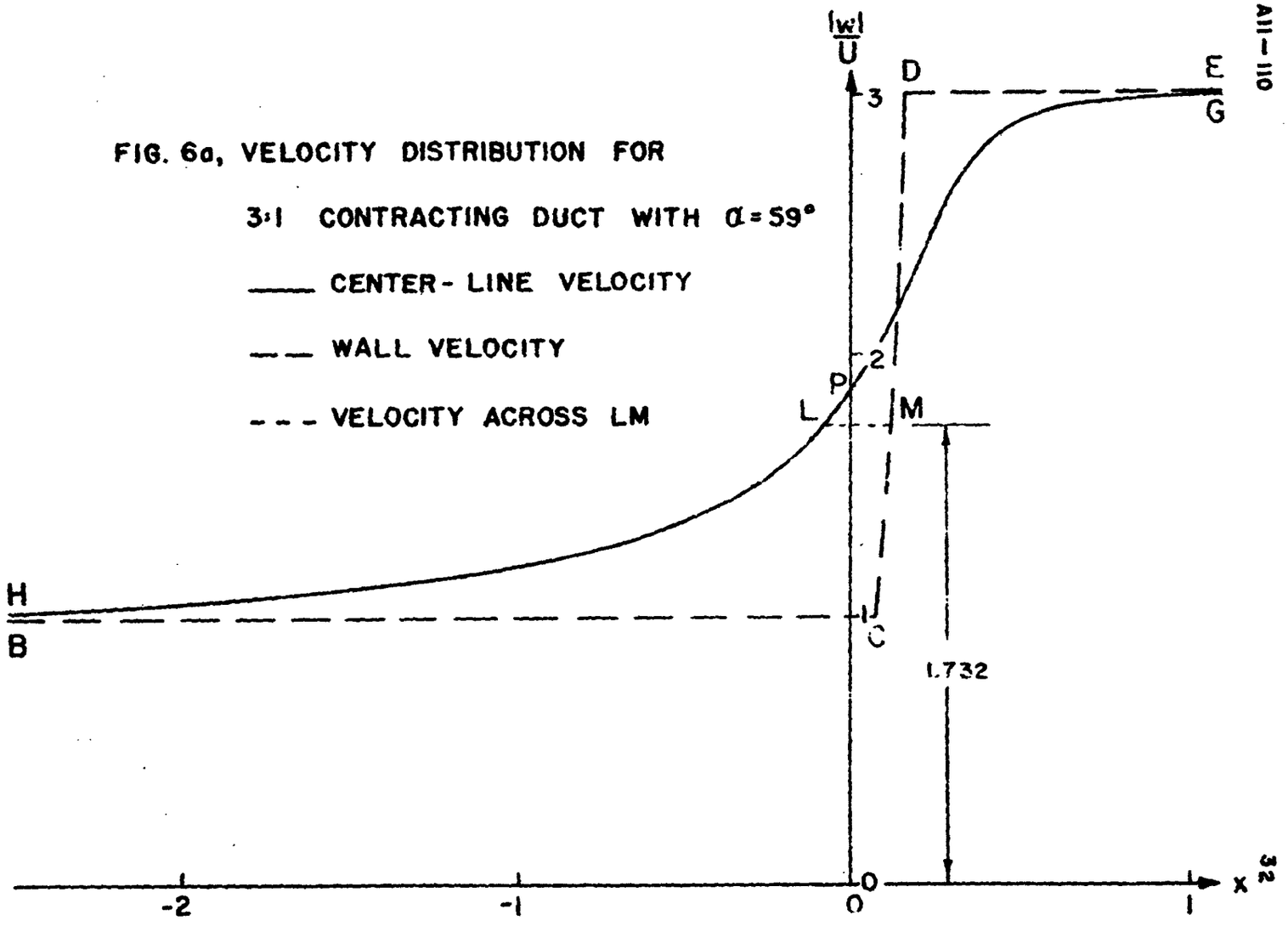

FIG. 6a, VELOCITY DISTRIBUTION FOR 3:1 CONTRACTING DUCT WITH $\alpha = 59°$

—— CENTER-LINE VELOCITY

– – WALL VELOCITY

– – – VELOCITY ACROSS LM

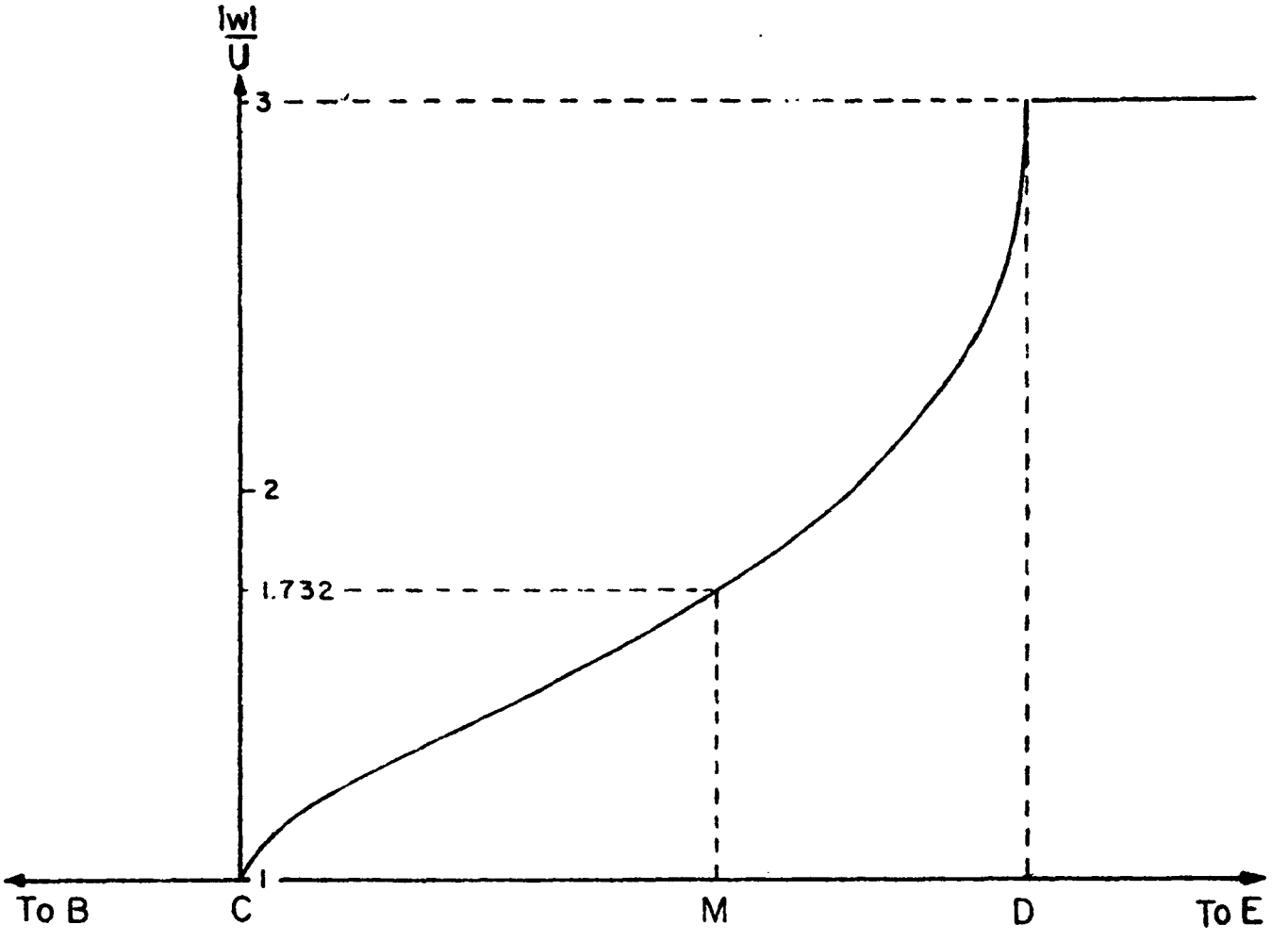

FIG. 6b, VELOCITY DISTRIBUTION ALONG CD FOR 3:1 CONTRACTING DUCT WITH $\alpha = 59°$

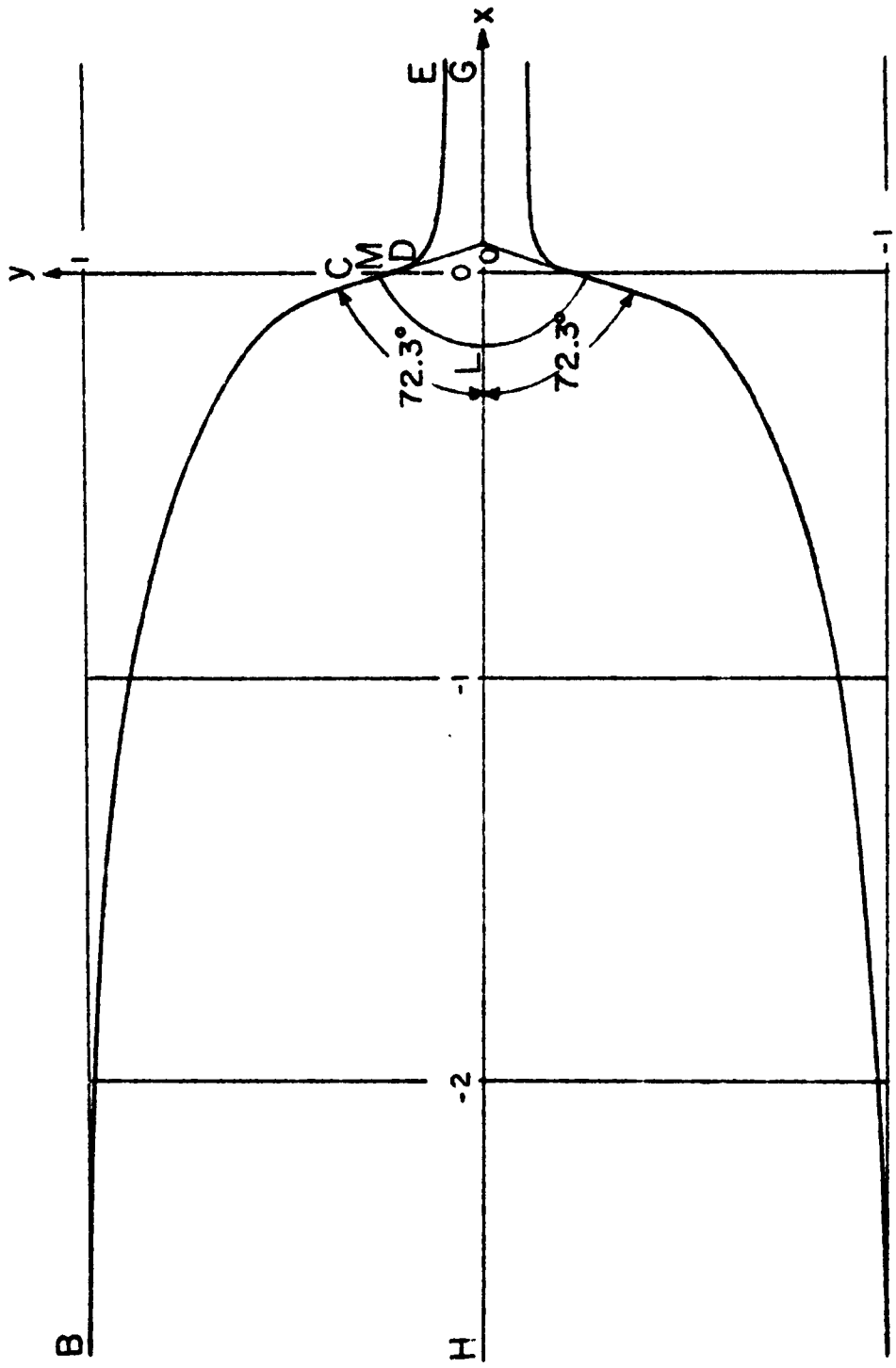

FIG. 7, CONTRACTING DUCT WITH $\alpha = \alpha_0$ (72.3°)

FIG. 7a, VELOCITY DISTRIBUTION FOR 10:1 CONTRACTING DUCT WITH $\alpha = 72.3°$

——— CENTER-LINE VELOCITY
— — WALL VELOCITY
- - - - - VELOCITY ACROSS L.M

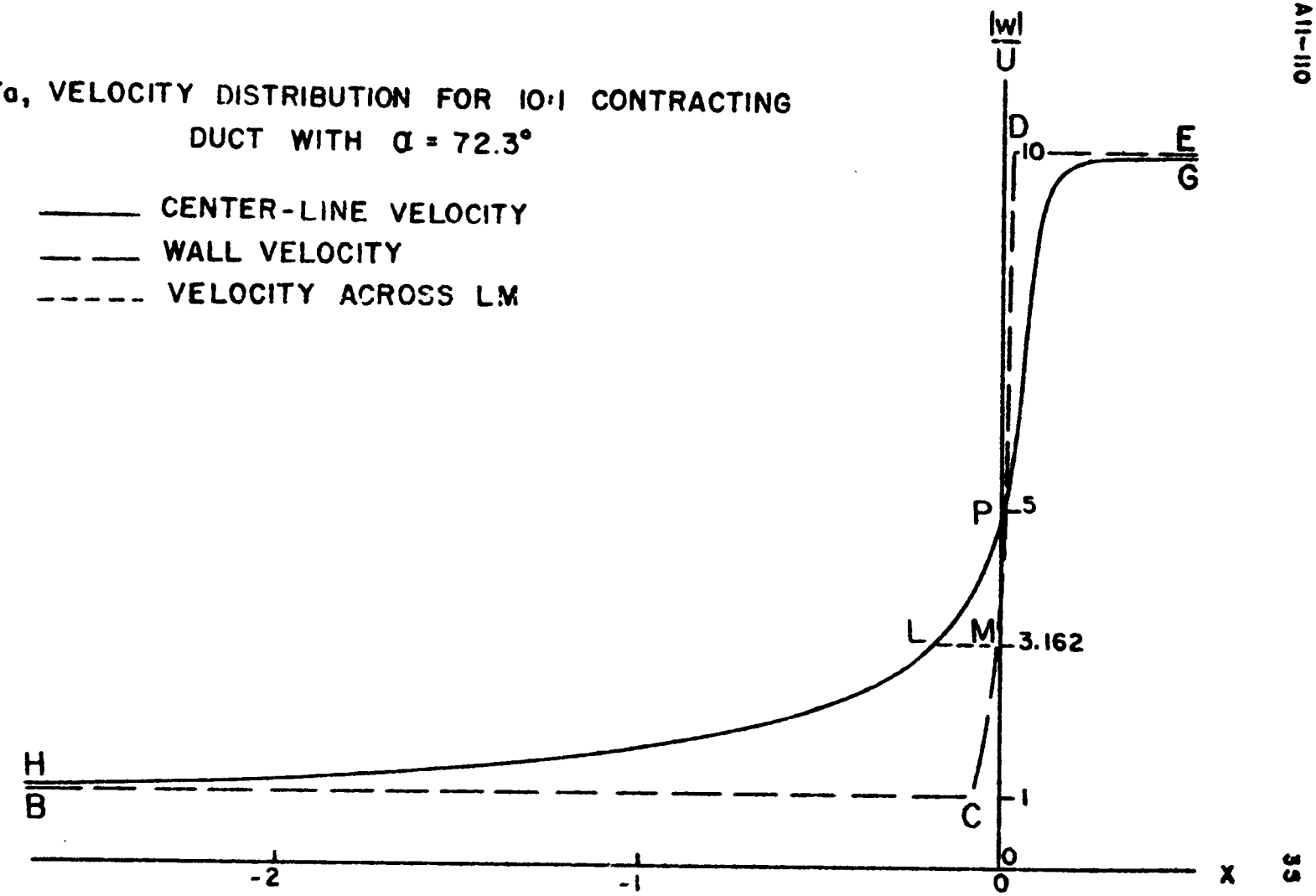

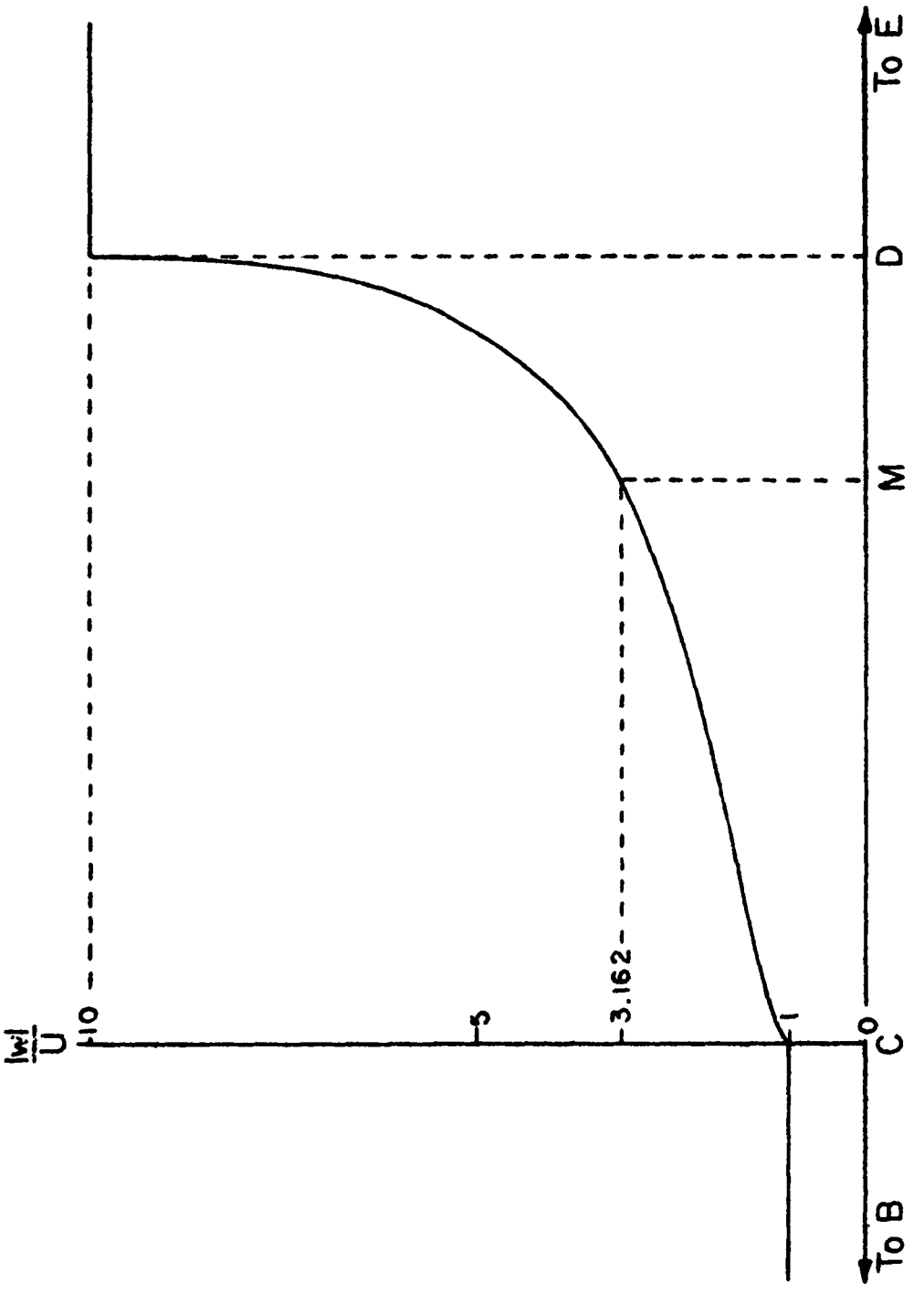

FIG. 7b, VELOCITY DISTRIBUTION ALONG CD FOR 10:1 CONTRACTING DUCT WITH $\alpha = 72.3°$